Mixed Membranes of Sphingolipids and Glycerolipids As Studied by Spin-Label ESR Spectroscopy. A Search for Domain Formation†

M. Pilar Veiga,‡ Félix M. Goñi,‡ Alicia Alonso,‡ and Derek Marsh*,§

Abteilung Spektroskopie, Max-Planck-Institut für biophysikalische Chemie, 37070 Göttingen, Germany, and Unidad de Biofísica (CSIC-UPV/EHU) and Departamento de Bioquímica, Universidad del País Vasco, Apartado 644, E-48080 Bilbao, Spain

Received March 24, 2000; Revised Manuscript Received June 7, 2000

ABSTRACT: The temperature dependences of the ESR spectra from different positional isomers of sphingomyelin and of phosphatidylcholine spin-labeled in their acyl chain have been compared in mixed membranes composed of sphingolipids and glycerolipids. The purpose of the study was to identify the possible formation of sphingolipid-rich in-plane membrane domains. The principal mixtures that were studied contained sphingomyelin and the corresponding glycerolipid phosphatidylcholine, both from egg yolk. Other sphingolipids that were investigated were brain cerebrosides and brain gangliosides, in addition to sphingomyelins from brain and milk. The outer hyperfine splittings in the ESR spectra of sphingomyelin and of phosphatidylcholine spin-labeled on C-5 of the acyl chain were consistent with mixing of the sphingolipid and glycerolipid components, in fluid-phase membranes. In the gel phase of egg sphingomyelin and its mixtures with phosphatidylcholine, the outer hyperfine splittings of sphingomyelin spin-labeled at C-14 of the acyl chain of sphingomyelin are smaller than those of the corresponding *sn*-2 chain spin-labeled phosphatidylcholine. This is in contrast to the situation with sphingomyelin and phosphatidylcholine spin-labeled at C-5, for which the outer hyperfine splitting is always greater for the spin-labeled sphingomyelin. The behavior of the C-14 spin-labels is attributed to a different geometry of the acyl chain attachments of the sphingolipids and glycerolipids that is consistent with their respective crystal structures. The two-component ESR spectra of sphingomyelin and phosphatidylcholine spin-labeled at C-14 of the acyl chain directly demonstrate a broad two-phase region with coexisting gel and fluid domains in sphingolipid mixtures with phosphatidylcholine. Domain formation in membranes composed of sphingolipids and glycerolipids alone is related primarily to the higher chain-melting transition temperature of the sphingolipid component.

In recent years, the idea of an in-plane heterogeneity of lipid and protein distribution in cell membranes has received growing experimental support (*1*). Such heterogeneity is favored, if not originated, in natural membranes by protein−protein and protein−lipid interactions (*2*). The presence of membrane regions with different compositions, i.e., domains, may be associated with specific cell functions. Some lipids may provide a favorable environment for a given protein, e.g., cardiolipin for cytochrome *c* oxidase (*3*, *4*); other proteins may be activated at the interfaces between domains (*5*), and some lipid domains may lead to membrane budding or invagination (*6*). Considerable attention is now being paid to the association between glycosylphosphatidylinositol (GPI)-anchored proteins and domains rich in sphingolipids, the so-called sphingolipid "rafts" (*7*−*9*).

It is important in this context to examine the role of lipid−lipid interactions in the formation of domains in the absence of proteins. For this purpose, model membranes consisting of pure lipids are particularly appropriate. Lipid domain formation may arise from a number of mechanisms, of which lateral phase separation of lipids with widely different chain-melting transition temperatures is a significant one. There is a considerable literature covering the behavior of binary mixtures of phosphoglycerolipids with different gel-to-fluid transition temperatures (see ref *10* for a review). This mechanism may be particularly relevant to the formation of sphingolipid-rich rafts because naturally occurring sphingolipids undergo chain melting near or above the physiological temperature region of 37 °C (*11*), whereas for most other membrane lipids, this transition occurs near or below 0 °C. Bar et al. (*12*), for example, have shown by a combination of fluorescence recovery after photobleaching, differential scanning calorimetry, and electron microscopy that chain mismatch in sphingomyelins with 24-carbon acyl chains can also lead to nonideal mixing with phosphatidylcholines.

Gel−fluid lateral phase separation can readily be detected in mixed lipid membranes from the well-resolved mobility differences in the electron spin resonance (ESR)[1] spectra of lipids that are spin-labeled in their acyl chains (*13*, *14*). Most information can be obtained from such studies when results from different spin-labeled lipid species in binary mixtures are compared (*15*). In principle, fluid−fluid phase separations

† This work was supported in part by Grant PB 96/0171 from DGICYT (Spain), Grant EX 98/10 from the Basque Government, and Grant UPV 042.310-G03/98 from the University of the Basque Country. M.P.V. is a predoctoral student supported by the Basque Government.

* To whom correspondence should be addressed: Abteilung Spektroskopie, Max-Planck-Institut für biophysikalische Chemie, 37070 Göttingen, Germany. Telephone: +49-551-201 1285. Fax: +49-551-201 1501. E-mail: dmarsh@gwdg.de.

‡ Universidad del País Vasco.

§ Max-Planck-Institut für biophysikalische Chemie.

10.1021/bi000678r CCC: $19.00
Published on Web 07/21/2000

may also be detected with this technique by analysis of the characteristic anisotropic rotational diffusion of the spin-labeled lipid chains (*16*).

In the work presented here, we have attempted to detect in-plane heterogeneities in lipid composition in pure lipid membranes composed of egg phosphatidylcholine and either egg or brain sphingolipids, with low or high degrees of chain mismatch, respectively. For that purpose, liposomes containing spin-labeled sphingomyelin or spin-labeled phosphatidylcholine have been examined by ESR spectroscopy. The investigation is complicated by the different spectral behavior of spin-labeled sphingomyelin and spin-labeled phosphatidylcholine which can be attributed to the different backbone and mode of chain attachment in sphingolipids and glycerolipids. In particular, mobility differences at the chain ends of the sphingolipid and glycerophospholipid in the gel phase are consistent with the different crystal structures of these two lipid classes. When allowance is made for this latter effect, lateral phase separation is detected in the sphingolipid−glycerolipid mixed membranes that corresponds to an inhomogeneous distribution of these two lipid components.

MATERIALS AND METHODS

Materials. Brain cerebrosides and egg and brain sphingomyelin were from Avanti Polar Lipids (Alabaster, AL), and milk sphingomyelin was from Matreya Inc. (Pleasant Gap, PA). Egg yolk phosphatidylcholine (grade I) was from Lipid Products (South Nutfield, England), and brain gangliosides were a gift from G. D. Fidelio (CONICET, Universidad Nacional de Córdoba, Córdoba, Argentina). Phosphatidylcholine spin-labels labeled at C-5 or C-14 in the stearoyl *sn*-2 chain of the lipid were synthesized as described previously (*17*). Sphingomyelin spin-labels labeled at the C-5 or C-14 position in the *N*-acyl chain were synthesized by the coupling reaction of the *N*-succinimidyl ester of spin-labeled stearic acid (*18*) with sphingosine-1-phosphocholine derived from bovine brain sphingomyelin (*19*).

Sample Preparation. Two micromoles of total lipids and 0.5 mol % spin-label were codissolved in chloroform or a 2:1 (v/v) chloroform/methanol mixture and evaporated under a stream of dry nitrogen gas. The residual solvent was removed by vacuum-drying overnight. The lipid film was then hydrated in 0.1 mL of 20 mM Hepes, 100 mM NaCl, and 1 mM EDTA (pH 7.4) by incubation for 1 h at 50 °C (80 °C for samples containing brain cerebrosides) with vortexing. Samples were then pelleted into a 1-mm inside diameter (i.d.) glass capillary; the excess supernatant was removed, and the capillary was flame-sealed.

ESR Measurements. ESR spectra were recorded on a Varian Century line 9 GHz spectrometer equipped with nitrogen gas flow temperature regulation. Samples in 1-mm i.d. glass capillaries were placed in a standard quartz ESR tube containing light silicone oil for thermal stability. Spectral data were collected digitally on a personal computer interfaced with the spectrometer, using software written by M. D. King of the Max-Planck-Institut. Outer hyperfine splittings ($2A_{max}$) were used to characterize the rotational disorder and rotational rates of the spin-labeled lipid chain segments (see ref *20*). For rotational mobility with components in the slow-motion regime (*21*), this parameter provides a useful comparative indicator of segmental mobility in equivalent systems (*14*).

RESULTS

Measurements have been performed with the sphingolipids egg sphingomyelin and brain cerebrosides, alone and in 1:1 molar mixtures with the glycerolipid egg phosphatidylcholine. The acyl chains of egg SM are predominantly palmitoyl (C16:0), and those of brain cerebrosides are for the most part lignoceroyl (C24:0). The majority *sn*-1 and *sn*-2 acyl chain species of egg PC are palmitoyl and oleoyl (C18:1), respectively. These chain compositions have a corresponding influence on the chain-melting phase behavior of the respective lipids. In addition, measurements were also made with a 4:1 molar mixture of egg sphingomyelin with brain gangliosides, both alone and in a 1:1 molar admixture with egg phosphatidylcholine. Appreciable formation of micelles occurs only at ganglioside contents higher than this (*22*). Throughout, results with the *n*-SMSL sphingomyelin spin-labels are compared with those of the corresponding *n*-PCSL phosphatidylcholine spin-labels. Spin-labels at C-5 of the acyl chain are used to investigate the behavior of the fluid phases because at this position of labeling they give ESR spectra with well-defined axial anisotropy that results from the dynamic chain ordering in the fluid phase. Spin-labels at C-14, close to the terminal methyl region of the acyl chains, are used to investigate the gel phase. These C-14 labels are also used to investigate the two-phase region of gel−fluid coexistence because they give close to optimum spectral resolution for the two lipid environments with glycerolipids.

5-Position Spin-Labels in the Fluid Phase. The ESR spectra of the 5-SMSL sphingomyelin spin-label and of the 5-PCSL phosphatidylcholine spin-label in fluid bilayer membranes composed of 1:1 (molar) mixtures of sphingolipids (egg SM or brain cerebroside) with egg PC and in the corresponding single-component lipid membranes are given in Figure 1. The ESR spectra all have an axially anisotropic line shape that is characteristic of such labels in fluid lipid bilayer membranes (*23*). Even for the mixed lipid membranes, the spectra are typical of a single lipid environment for the two spin-labels in the fluid phase. In all cases, the anisotropy and outer hyperfine splittings in the spectra of the spin-labeled sphingomyelin are greater than those of the corresponding phosphatidylcholine spin-label. These spectral differences trace back to the molecular differences in the lipid backbone and mode of chain attachment between sphingolipids and glycerolipids (*24*).

The temperature dependences of the outer hyperfine splittings ($2A_{max}$) for the 5-SMSL and 5-PCSL spin-labels in the various sphingolipid and glycerolipid host membranes are given in Figure 2. The larger values of $2A_{max}$ for 5-SMSL than for 5-PCSL are evident throughout the temperature range studied for all host membranes. Bilayer membranes

[1] Abbreviations: *n*-SMSL, *N*-[*n*-(4,4-dimethyloxazolidine-*N*-oxyl)-stearoyl]sphingosine-1-phosphocholine; *n*-PCSL, 1-acyl-2-[*n*-(4,4-dimethyloxazolidine-*N*-oxyl)stearoyl]-*sn*-glycero-3-phosphocholine; SM, egg sphingomyelin; BSM, bovine brain sphingomyelin; CB, brain cerebrosides; Gg, brain gangliosides; PC, phosphatidylcholine; Hepes, *N*-(2-hydroxyethyl)piperazine-*N*′-2-ethanesulfonic acid; EDTA, ethylenediaminetetraacetic acid; ESR, electron spin resonance.

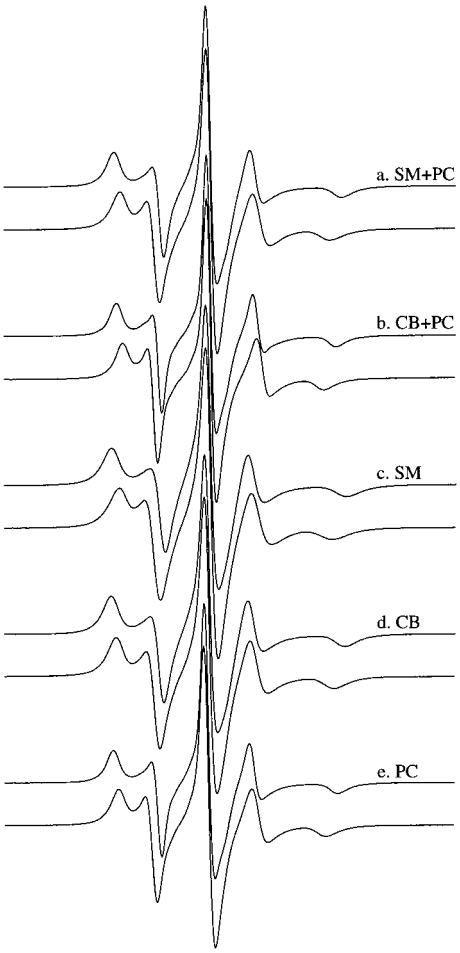

FIGURE 1: ESR spectra of the 5-SMSL sphingomyelin spin-label (upper spectrum of each pair) and of the 5-PCSL phosphatidylcholine spin-label (lower spectrum of each pair) in fluid bilayer membranes of (a) a 1:1 (molar) egg SM/egg PC mixture at 50 °C, (b) a 1:1 (molar) brain CB/egg PC mixture at 70 °C, (c) egg sphingomyelin at 50 °C, (d) brain cerebroside at 70 °C, and (e) egg PC at 50 °C. The total scan width was 100 G.

of egg PC alone are in a fluid liquid−crystalline state throughout the entire temperature range (4−80 °C). Bilayers of egg SM alone undergo a chain-melting phase transition from a gel to a fluid state in the region between 33 and 37 °C, in reasonable agreement with results from differential scanning calorimetry (T_t = 38 °C, $\Delta T \sim 2$ °C; data not shown). Membranes composed of brain cerebrosides alone undergo a chain-melting phase transition at higher temperatures, in the region of 50−60 °C.

The temperature dependences of the spin-label spectra from the sphingolipid/glycerolipid mixtures give little evidence for a pronounced thermotropic phase transition over the range of temperatures that was studied. As will be seen later, a broad range of phase coexistence occurs in the low-temperature regime. At higher temperatures, in the fluid phase, the outer hyperfine splittings in the mixtures are intermediate between the values for the phosphatidylcholine component alone and those of the sphingolipid alone. This is true for both the sphingomyelin and the phosphatidylcholine spin-labels, which suggests that the sphingolipid and glycerolipid components mix reasonably well together in the fluid-phase membranes. The mean values of $2A_{max}$ that are calculated from the single-component values for a 1:1 (molar) mixture of egg SM with PC, and of CB with PC, are given

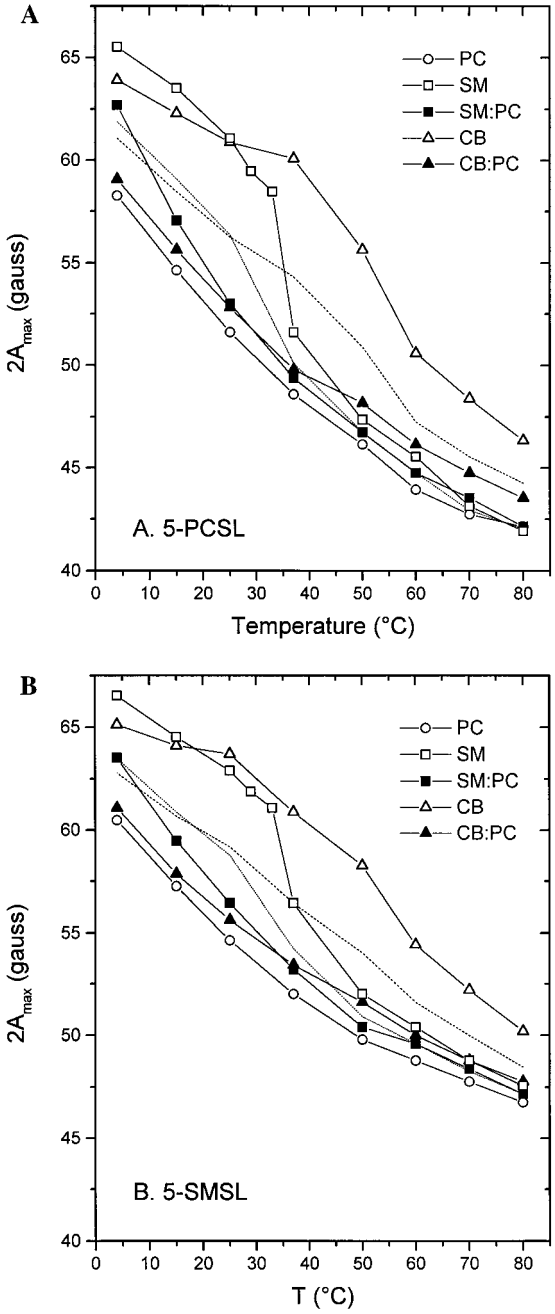

FIGURE 2: Temperature dependence of the outer hyperfine splittings, $2A_{max}$, of (A) the 5-PCSL phosphatidylcholine spin-label and (B) the 5-SMSL sphingomyelin spin-label, in bilayer membranes of egg PC (○), egg SM (□), a 1:1 (molar) egg SM/egg PC mixture (■), brain cerebroside (△), and a 1:1 (molar) brain CB/egg PC mixture (▲). The lines without symbols correspond to mean values for the single lipids and refer to the single-lipid pairs SM and PC [1:1 (molar)] and CB and PC [1:1 (molar)] (see the text).

by the lines without symbols in panels A and B of Figure 2. With the exception of 1:1 (molar) egg SM and PC at 4 °C, the values measured experimentally with these lipid mixtures either lie below or are coincident with the mean value, for both the 5-SMSL and 5-PCSL spin-labels. This would not be the case if 5-SMSL were sampling a preferentially sphingolipid-enriched phase. The most likely interpretation is that on mixing, the interactions between the sphingolipid and phosphatidylcholine produce a more homogeneous phase in which the lipid chain mobility is intermediate between that of egg PC alone and the sphingolipid (egg SM or CB) alone, in the fluid phase. In the mixture with the higher

Table 1: Differences in Outer Hyperfine Splitting, $2\Delta A_{max}^{(i)}$, in the ESR Spectra of the 5-SMSL and 5-PCSL Spin-Labels between Mixed Sphingolipid/Glycerolipid Membranes in the Fluid Phase and Those Composed Only of the Corresponding Glycerolipid (i.e., egg PC alone), *i*[a]

	37 °C		50 °C	
membrane[b]	5-SMSL	5-PCSL	5-SMSL	5-PCSL
(SM+PC)-PC[c]	0.27	0.27	0.27	0.50
(SM+Gg+PC)-PC[c]	0.22	0.20	0.55	0.25
(SM+CB+PC)-PC[c]	0.35	0.32	0.41	0.35
(BSM+PC)-PC[c]	0.44	0.36	0.58	0.39
	70 °C		80 °C	
	5-SMSL	5-PCSL	5-SMSL	5-PCSL
(CB+PC)-PC[c]	0.23	0.36	0.29	0.33

[a] The differences are normalized to those $[2\Delta A_{max}^{(i,j)}]$ between glycerolipid and sphingolipid systems *i* and *j*. [b] SM+PC, 1:1 (molar) mixture; the complement corresponding to 1.0 minus the values given is with SM (as opposed to PC), taken as a reference state. SM+Gg+PC, 4:1:5 (molar) mixture; complement SM+Gg 4:1 (molar) mixture. SM+CB+PC, 1:1:2 (molar) mixture; complement SM+CB 1:1 (molar) mixture. BSM+PC, 1:1 (molar) mixture; complement BSM. CB+PC, 1:1 (molar) mixture; complement CB. [c] Values for the complementary differences, e.g., SM-(SM+PC), are simply 1 minus the values given [i.e., $[\Delta A_{max}^{(i)} + \Delta A_{max}^{(j)}]/\Delta A_{max}^{(i,j)} = 1$].

melting of the two sphingolipids (i.e., CB), the chain mobility is closer to that of the glycerolipid component (PC) alone.

Quantitatively, the differences in the outer hyperfine splittings of the 5-SMSL or 5-PCSL spin-labels between the fluid phases of the mixed lipid systems and the corresponding single-glycerolipid system (i.e., egg PC) are given in Table 1, for a range of sphingolipid/glycerolipid mixtures. The values that are tabulated are the differences, $2\Delta A_{max}^{(i)}$, in $2A_{max}$ between the mixed systems and the glycerolipid-alone system *i*. These values are normalized to the difference, $2\Delta A_{max}^{(i,j)}$, in $2A_{max}$ between the sphingolipid-alone and glycerolipid-alone components, *i* and *j*, of the mixtures. This normalization is necessary because of the intrinsic difference between the outer hyperfine splittings of the 5-SMSL and 5-PCSL spin-labels (see above). The meaning of the values calculated in this way is explained in the Appendix. Even after normalization, these differences for the two spin-labels are generally not very greatly different, for any of the sphingolipid/glycerolipid mixtures that have been studied. This again suggests that there are not independent fluid phases that are preferentially enriched in either the sphingolipid or glycerolipid component, but rather that these two lipid components mix and mutually interact in the fluid phase (see the Discussion).

14-Position Spin-Labels in the Gel Phase. The ESR spectra of the 14-SMSL sphingomyelin spin-label and the 14-PCSL phosphatidylcholine spin-label in bilayer membranes of egg SM, brain cerebrosides, and their 1:1 (molar) mixtures with egg PC, at low temperature in the gel phase, are given in Figure 3. The spectra from egg SM and brain CB alone correspond to the slow-motion regime of conventional nitroxide spin-label ESR spectroscopy that is typical for gel-phase lipids (*23*). The spectra from the lipid mixtures with egg PC consist primarily of a slow-motion component that is characteristic of the gel phase [seen most clearly in the spectrum of 14-PCSL in 1:1 (molar) SM/PC membranes]. However, these spectra from the lipid mixtures contain additionally a component corresponding to the intermediate-motion regime, indicating that these samples are already in a two-phase region at low temperatures (see below).

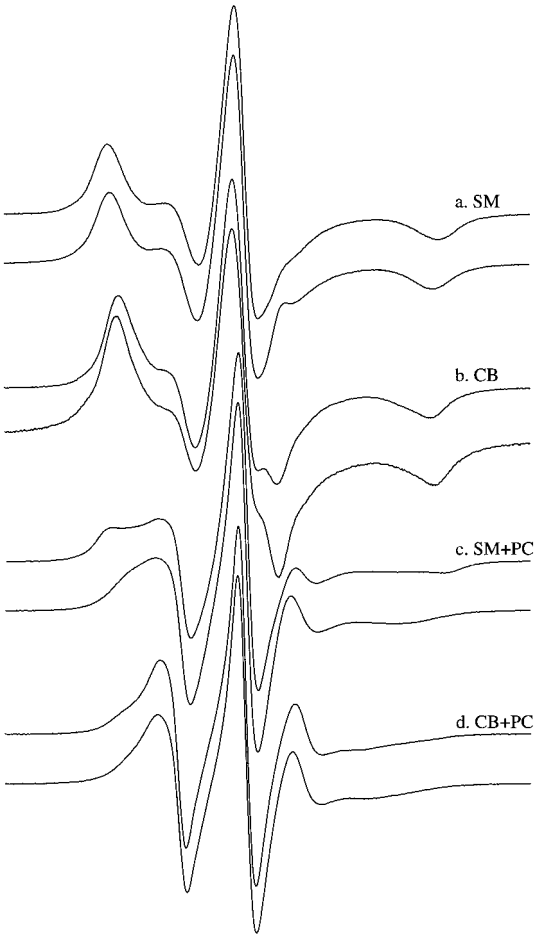

FIGURE 3: ESR spectra of the 14-SMSL sphingomyelin spin-label (lower spectrum of each pair) and of the 14-PCSL phosphatidylcholine spin-label (upper spectrum of each pair) in gel-phase bilayer membranes of (a) egg sphingomyelin at 4 °C, (b) brain cerebroside at 4 °C, (c) a 1:1 (molar) egg SM/egg PC mixture at 1 °C, and (d) a 1:1 (molar) brain CB/egg PC mixture at 4 °C. The total scan width was 100 G.

A highly significant feature that is seen consistently in the spectra of samples containing egg sphingomyelin is that the outer hyperfine splitting of the gel-phase component of the 14-SMSL spin-labeled sphingomyelin is considerably smaller than that of the 14-PCSL spin-labeled phosphatidylcholine. This effect is particularly pronounced in the mixture with egg PC, and contributes to the poorer spectral resolution of the gel and fluid lipid components of 14-SMSL compared with that of 14-PCSL (see Figure 3c). These results are in contrast to those obtained from the 5-position spin-labels in the fluid phase, for which the outer hyperfine splitting of 5-SMSL is greater than that of 5-PCSL. The latter is a general result for all positions of labeling in the fluid phase (*24*). Even 14-SMSL exhibits a lower mobility than 14-PCSL in the fluid phases examined here (spectra not shown).

The outer hyperfine splittings, $2A_{max}$, of the 14-SMSL and 14-PCSL spin-labels in the gel phases of various sphingolipids and their mixtures with egg PC are given in Table 2. This includes data corresponding to the spectra shown in Figure 3 and, in addition, measurements on mixtures of brain

Table 2: Outer Hyperfine Splittings, $2A_{max}$ (gauss), in the ESR Spectra of the 14-SMSL Sphingomyelin and 14-PCSL Phosphatidylcholine Spin-Labels in Mixed Membranes, and Single-lipid Controls, Composed of Sphingolipids (egg sphingomyelin, SM; brain cerebrosides, CB; brain gangliosides, Gg) and Egg Phosphatidylcholine (PC)[a]

	4 °C		10 °C		15 °C	
membrane	14-SMSL	14-PCSL	14-SMSL	14-PCSL	14-SMSL	14-PCSL
SM	61.7	63.1	59.7	61.9	56.7	60.9
SM:PC (1:1)	53.6	62.9	49.6	63.1	38.1	63.7
CB	61.1	59.9	59.9	58.7	60.1	57.5
CB:PC (1:1)	51.0	53.2	38.5	37.1	37.3	35.7
SM:Gg (4:1)	61.9	63.3	59.5	61.3	(57.1)	62.3
SM:Gg:PC (4:1:5)	53.4	62.3	52.6	58.7	38.9	35.9

[a] Measurements were made in the gel phase of the sphingolipid component at the temperatures indicated.

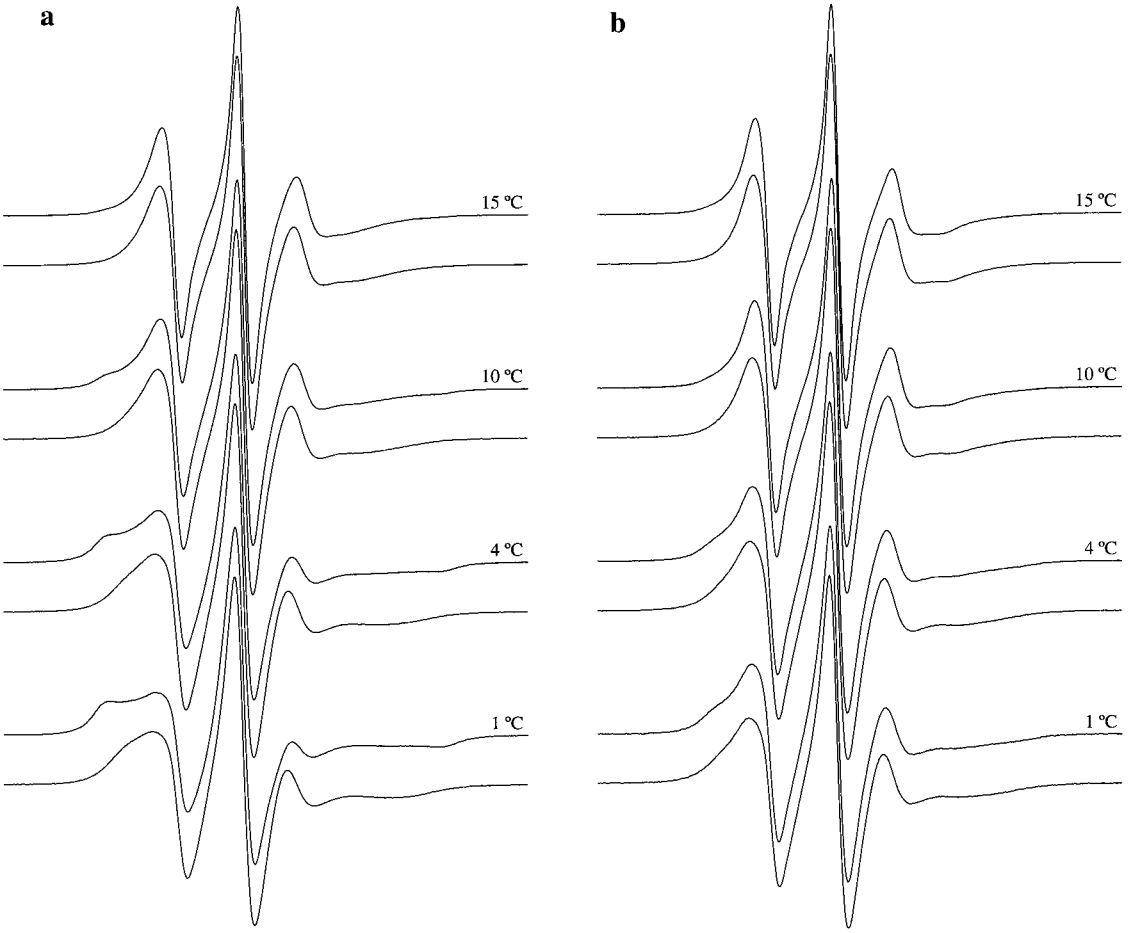

FIGURE 4: Temperature dependence of the ESR spectra of the 14-SMSL sphingomyelin spin-label (lower spectrum of each pair) and of the 14-PCSL phosphatidylcholine spin-label (upper spectrum of each pair) in membranes of (a) a 1:1 (molar) egg SM/egg PC mixture and (b) a 1:1 (molar) brain CB/egg PC mixture, in the two-phase region. The total scan width was 100 G.

gangliosides with egg SM. With the exception of the cerebroside-containing systems, the smaller outer hyperfine splitting of 14-SMSL, compared with that of 14-PCSL, is a common feature of the sphingolipid systems that have been studied. This anomalous behavior of the 14-position labels in the gel phase, as compared with that in the fluid phase, is related to the packing of the chain ends in the crystal structures of sphingolipids, as discussed later.

Two-Phase Region. As already noted (cf. Figure 3), the ESR spectra of the 14-position labels provide clear evidence for gel−fluid phase coexistence in the sphingolipid/glycerolipid mixtures, at the lowest temperatures that were investigated. The ESR spectra of the 14-SMSL and 14-PCSL spin-labels in the lipid mixtures, over a broader range of temperatures and phase coexistence, are given in Figure 4. Phase coexistence is evident in the spectra of 14-PCSL in a 1:1 (molar) egg SM/egg PC mixture from <1 to ∼15 °C (Figure 4a). As the temperature increases, not only do the line shapes of the individual spectral components change in the direction expected for increasing lipid mobility but also the relative population of the fluid lipid component increases at the expense of the gel-phase component. By 15 °C, the broad gel-phase spectral component is just visible in the outer wings of the sharper, almost three-line, fluid lipid spectral component. This type of gel−fluid phase separation is that expected for mixtures of a sphingolipid with a glycerolipid of lower chain-melting transition temperature (<0 °C for egg PC).

For 14-SMSL in a 1:1 (molar) egg SM/egg PC mixture at 1−4 °C, the two-component nature of the spectra that arises

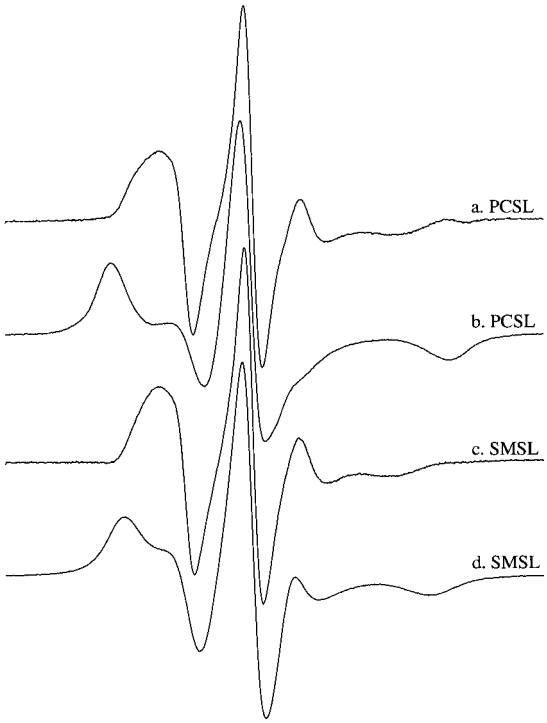

FIGURE 5: ESR difference spectroscopy. (a) Difference spectrum obtained by subtracting spectrum b from the spectrum of 14-PCSL in a 1:1 (molar) egg SM/egg PC mixture at 1 °C. (b) Spectrum of 14-PCSL in egg SM alone at 4 °C. (c) Difference spectrum obtained by subtracting spectrum d from the spectrum of 14-SMSL in a 1:1 (molar) egg SM/egg PC mixture at 1 °C. (d) Spectrum of 14-SMSL in egg SM alone at 15 °C. The total scan width was 100 G.

from the gel−fluid phase coexistence is readily discernible from the shoulders in the outer wings (see Figure 4a). However, for the reasons given previously, the resolution of the two spectral components is not as good as that for 14-PCSL. As a consequence, the two spectral components rapidly become indistinguishable at higher temperatures. A similar effect is observed in the ESR spectra of the two spin-labels in membranes of egg SM alone (data not shown). Whereas two-component spectra are visible from 25 to 35 °C for 14-PCSL in egg SM membranes, poorly resolved two-component spectra are only visible over a more limited temperature range about 30 °C for 14-SMSL in this membrane system. Effects comparable to those for egg SM plus egg PC (Figure 4a) are seen also in the two-component spectra of the 14-PCSL and 14-SMSL spin-labels in 1:1 (molar) brain CB/egg PC mixtures that are given in Figure 4b.

The lack of resolution of the two components makes spectral subtractions (to quantitate their relative intensities) difficult in the case of 14-SMSL. This is a restriction inherent to the system and is caused by the smaller spectral splittings of the spin-labeled sphingolipid in the gel phase (cf. Table 2). The results of spectral subtractions for 1:1 (molar) mixed membranes of egg SM and egg PC at 1 °C are given in Figure 5. Digital subtractions are performed by using single-component spectra from egg SM alone in the gel phase at a temperature giving nearest matching of the gel-phase component in the spectra of the lipid mixture (see the legend of Figure 5). Approximately 60−65% of the total intensity is contributed by the gel-phase spectral component for both the 14-SMSL and 14-PCSL labels, despite their different spectral line shapes. On the basis of the phase rule, one would expect a higher proportion of the higher-melting component than of the lower-melting component to be present in the gel phase. Reasons for this apparent discrepancy may be that the spin-labeled sphingomyelin and phosphatidylcholine do not faithfully reflect the distribution of the unlabeled counterparts because of differences in chain composition. (It will be noted that the host lipids, being of natural origin, also possess some heterogeneity in chain composition.) Finally, some margin of uncertainty must be included in the subtraction results for 14-SMSL because of the poorer resolution of the two spectral components. It is difficult to estimate what the relative weights of this and of the effects of chain heterogeneity are likely to be.

DISCUSSION

Fluid Phase. The spectra of the 5-position labels (see Figure 1), and of the 14-position labels (not shown), in the fluid phases of the lipid mixtures consist of a single component. This is consistent with a homogeneous fluid phase, but does not completely preclude the possibility of fluid−fluid phase separation. If the spectral differences between two putative fluid phases, in terms of frequencies, are on the same order as, or less than, the frequency of lipid exchange between these phases by translational diffusion, then a homogeneous motionally averaged single-component spin-label ESR spectrum would be obtained (*25*).

A possible model, which is consistent with the analysis of the hyperfine splittings that was given in the Results, is one of fast exchange between putative phase-separated domains that consist solely either of sphingolipid or of glycerolipid. A general version of such a model is analyzed in the Appendix. In this particular case, the hyperfine splittings intrinsic to the putative phase-separated environments are simply those observed for the corresponding single lipid components, i.e., sphingolipid and glycerolipid alone. For the 1:1 mixtures, the fractional populations of the phase-separated domains must be equal. However, if the spin-labeled sphingomyelin and phosphatidylcholine directly reflect the distribution of the sphingolipid and glycerolipid components in the putative phase-separated fluid lipid mixture, it would be expected that the spin-label populations would be very strongly biased to one of the phases, i.e., $f_i \approx 1$ and $f_j \approx 0$ or vice versa (see the Appendix). This is clearly not the case for the normalized differences in hyperfine splittings that are given in Table 1, and which should represent the relative spin-label populations (see the Appendix). Rather, these values are comparable for the spin-labeled sphingolipid and glycerolipid, and also are not equal to one-half, which would be expected for the opposite extreme of a uniform distribution of the labels between the two putative phases in the 1:1 mixtures. It is possible that the putative fluid−fluid phase separation could involve phases of more complex composition, but still it would be expected that the normalized difference in hyperfine splittings, $\Delta A_{max}^{(i)}/\Delta A_{max}^{(i,j)}$, would be more different for the spin-labeled sphingolipid and glycerolipid components. The most likely interpretation of the results given in Table 1 is therefore that the sphingolipid and glycerolipid components are mixing and mutually interacting in the fluid phase of these mixed lipid systems. Hence, it is concluded that a pronounced phase

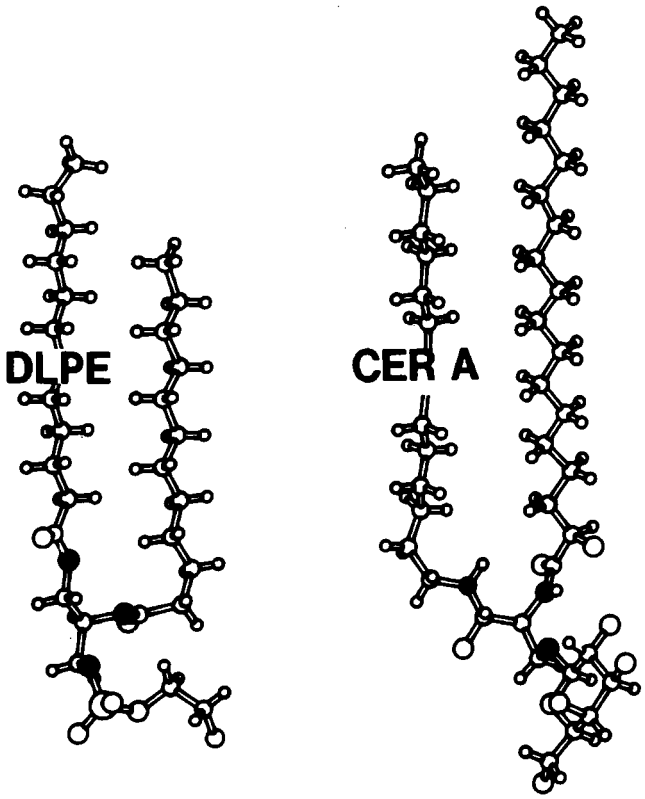

FIGURE 6: Chain stacking in the crystal structures of glycerolipids and sphingolipids: (left) dilauroylphosphatidylethanolamine (DLPE) and (right) galactosyl *N*-hydroxystearoyl cerebroside (CER A). Adapted from Pascher et al. (*26*), with permission from Elsevier Science.

separation of sphingolipids and glycerolipids is unlikely to occur in the fluid phase of their mixtures.

Gel Phase. The characteristic feature of the 14-position spin-labels in the gel phase of egg SM is that the outer hyperfine splitting of the spin-labeled sphingomyelin is smaller than that of the spin-labeled phosphatidylcholine (Table 2). Whereas the opposite situation (which is the usual case) can be explained in terms of the different chain linkage at the lipid backbone (*24*), this unusual result points to structural differences in the region of the chain ends. The situation is illustrated in Figure 6 in which the crystal structure of the sphingolipid galactosyl *N*-stearoyl cerebroside is compared with the archetypal glycerolipid crystal structure of dilauroylphosphatidylethanolamine. For glycerolipids which usually have the (+)-syn-clinal conformation for the *sn*-1 chain, the *sn*-2 acyl chain (which is spin-labeled) is effectively shorter than the *sn*-1 chain (*26*). Carbon atoms of the *sn*-2 glycerolipid chain are located approximately three CH_2 units higher than those in numerically equivalent positions of the *sn*-1 acyl chain. For the sphingolipids, the backbone conformation of which is biased more in the direction of an *sn*-2 syn-clinal conformation for a corresponding glycerolipid, the *N*-acyl chain (which is spin-labeled) is effectively longer than the partner sphingosine chain (see Figure 6). This is because the segment from C-1 to C-5, or C-6, of the sphingosine chain is in an all-*trans* configuration with the amide plane nearly perpendicular, and beyond this, the sphingosine chain is bent to be approximately parallel with the *N*-acyl chain. Equivalent positions in the *N*-acyl chain are thus shifted by approximately four CH_2 units downward with respect to the sphingosine chain, bringing C-14 of the *N*-stearoyl chain into the region of the terminal methyl group of the C_{18} sphingosine. This comparison therefore suggests that the chain configuration of the sphingomyelin spin-label in the gel phase is similar to that of the cerebroside crystal structure, and that the higher mobility at the chain end correspondingly arises from the lack of intramolecular chain overlap for the *N*-acyl chain, which is more analogous to that of the *sn*-1 chain in glycerolipids. Recent deuterium NMR studies have concluded that the configuration of the chain linkage in the fluid phase of cerebrosides is also similar to that in the crystal (*27*).

The discrepancy between 14-SMSL and 14-PCSL is less marked in other sphingolipid systems, and even inverted in brain cerebroside host lipids (Figure 3b), which have considerably longer *N*-acyl chains. Indeed, there is a pronounced dependence of this effect on the chain composition of the sphingolipid host, also among different sphingomyelins. For bovine brain sphingomyelin which has predominantly C18:0 *N*-acyl chains, it is found that the outer hyperfine splittings are rather similar for the 14-SMSL and 14-PCSL spin-labels in the gel phase. On the other hand, for milk sphingomyelin which has a mixture of *N*-acyl chains, it is found that the outer hyperfine splittings are larger for 14-PCSL, just as for egg SM in the gel phase (data not shown).

Gel−Fluid Coexistence. It was found above that sphingolipids and glycerolipids most probably mix reasonably well in fluid-phase membranes. The situation at lower temperatures is, however, different because the chain-melting transition temperatures of natural sphingolipids, unlike those of natural glycerolipids, can lie appreciably above physiological temperatures (see Figure 2 for cerebrosides). Direct evidence for the coexistence of gel and fluid domains was found from the two-component ESR spectra that were obtained from the 14-position spin-labeled lipids. Unfortunately, for technical reasons that have already been discussed, quantification of the ESR spectra from spin-labeled sphingomyelin could not be performed with great accuracy. Nevertheless, it seems likely that the gel-phase domains are preferentially enriched in the higher-melting component, i.e., in the sphingolipid, as is expected from general considerations of the phase rule. In the absence of membrane components other than sphingolipids and glycerolipids, it is in this classical thermodynamic sense that the sphingolipid component of membranes has the propensity to form differentiated in-plane domains. A similar conclusion has been reached from studies on the solubility of lipid mixtures in detergent at low temperature (*28*), i.e., the standard biochemical method used for identification and isolation of compositionally enriched cell membrane "domains". The results presented here form a rational basis on which to search for the mechanism by which other membrane components may stabilize or potentiate formation of sphingolipid microdomains, or rafts, in cellular membranes.

This is, in principle, a viable in vivo mechanism because, as already mentioned and demonstrated here, sphingolipids of natural origin have chain-melting temperatures in the physiological range or higher.

ACKNOWLEDGMENT

We thank Frau B. Angerstein for the preparation of spin-labeled phospholipids, Drs. P. Hoffmann and K. Sandhoff

for samples of spin-labeled sphingomyelin, and Dr. G. B. Fidelio for the gift of brain gangliosides.

APPENDIX

Motionally Averaged Hyperfine Splittings for Fast Exchange. For a spin-labeled lipid in fast exchange between two different environments, the motionally averaged outer hyperfine splitting, $2A_{max}$, that is observed is simply the weighted average of those for the two separate lipid environments *i* and *j* (*25*):

$$A_{max} = f_i A_{max}^{(i)} + f_j A_{max}^{(j)} \quad \text{(A1)}$$

where f_i and f_j are the fractional populations of the spin-label in the two lipid environments *i* and *j*, respectively ($f_i + f_j = 1$), and $A_{max}^{(i)}$ and $A_{max}^{(j)}$ are the respective hyperfine splitting constants intrinsic to these environments. The differences in outer hyperfine splitting between the two-phase and single-phase systems are then given by

$$A_{max}^{(i)} - A_{max} = f_j[A_{max}^{(i)} - A_{max}^{(j)}] \quad \text{(A2)}$$

$$A_{max} - A_{max}^{(j)} = f_i[A_{max}^{(i)} - A_{max}^{(j)}] \quad \text{(A3)}$$

Hence, the normalized differences should be $\Delta A_{max}^{(i)}/\Delta A_{max}^{(i,j)} = f_j$ and $\Delta A_{max}^{(j)}/\Delta A_{max}^{(i,j)} = f_i$, where $\Delta A_{max}^{(i,j)} = A_{max}^{(i)} - A_{max}^{(j)}$. $\Delta A_{max}^{(i)}$ and $\Delta A_{max}^{(j)}$ are the left-hand side of eqs A2 and A3, respectively, as defined in the text. A specific model of this type that is tested here is one in which the two environments are composed solely of one lipid type (e.g., sphingolipid or glycerolipid) in a binary mixture. The hyperfine splitting constants $A_{max}^{(i)}$ and $A_{max}^{(j)}$ can then be obtained directly from measurements on the single-component systems.

REFERENCES

1. Bergelson, L. D. (1995) *Mol. Membr. Biol. 12*, 125−129.
2. Welti, R., and Glaser, M. (1994) *Chem. Phys. Lipids 73*, 121−137.
3. Powell, G. L., Knowles, P. F., and Marsh, D. (1985) *Biochim. Biophys. Acta 816*, 191−194.
4. Abramovitch, D. A., Marsh, D., and Powell, G. L. (1990) *Biochim. Biophys. Acta 1020*, 34−42.
5. Basáñez, G., Nieva, J. L., Goñi, F. M., and Alonso, A. (1996) *Biochemistry 35*, 15183−15187.
6. Lipowsky, R. (1993) *Biophys. J. 64*, 1133−1138.
7. Brown, D. A., Crise, B., and Rose, J. K. (1989) *Science 245*, 1499−1501.
8. Brown, D. A., and Rose, J. K. (1992) *Cell 68*, 533−544.
9. Simons, K., and Ikonen, E. (1997) *Nature 387*, 569−572.
10. Marsh, D. (1990) *Handbook of Lipid Bilayers*, 387 pp, CRC Press, Boca Raton, FL.
11. Barenholz, Y. (1984) in *Physiology of Membrane Fluidity* (Shinitzki, M., Ed.) Vol. 1, pp 131−173, CRC Press, Boca Raton, FL.
12. Bar, L. K., Barenholz, Y., and Thompson, T. E. (1997) *Biochemistry 36*, 2507−2516.
13. Heimburg, T., Würz, U., and Marsh, D. (1992) *Biophys. J. 63*, 1369−1378.
14. Rama Krishna, Y. V. S., and Marsh, D. (1990) *Biochim. Biophys. Acta 1024*, 89−94.
15. Schorn, K., and Marsh, D. (1996) *Biochemistry 35*, 3831−3836.
16. Wu, S. H., and McConnell, H. M. (1975) *Biochemistry 14*, 847−854.
17. Marsh, D., and Watts, A. (1982) in *Lipid−Protein Interactions* (Jost, P. C., and Griffith, O. H., Eds.) Vol. 2, pp 53−126, Wiley-Interscience, New York.
18. Lapidot, Y., Rappoport, S., and Wolman, Y. (1967) *J. Lipid Res. 8*, 142−145.
19. Barenholz, Y., and Gatt, S. (1982) in *Phospholipids* (Hawthorne, A., Ed.) pp 129−177, Elsevier Biomedical Press, Amsterdam.
20. Marsh, D. (1982) in *Techniques in Lipid and Membrane Biochemistry* (Metcalfe, J. C., and Hesketh, T. R., Eds.) Vol. B4/II, B426, pp 1−44, Elsevier, Amsterdam.
21. Moser, M., Marsh, D., Meier, P., Wassmer, K.-H., and Kothe, G. (1989) *Biophys. J. 55*, 111−123.
22. Barenholz, Y., Ceastaro, B., Lichtenberg, D., Freire, E., Thompson, T. E., and Gatt, S. (1980) in *Advances in Experimental Medicine and Biology. Structure and Function of Gangliosides* (Svennerholm, L., Mandel, P., Dreyfus, H., and Urban, P.-F., Eds.) Vol. 125, pp 105−123, Plenum Press, New York.
23. Marsh, D. (1981) in *Membrane Spectroscopy. Molecular Biology, Biochemistry and Biophysics* (Grell, E., Ed.) Vol. 31, pp 51−142, Springer-Verlag, Berlin.
24. Hoffmann, P., Sandhoff, K., and Marsh, D. (2000) *Biochim. Biophys. Acta* (in press).
25. Marsh, D., and Horváth, L. I. (1989) in *Advanced EPR. Applications in Biology and Biochemistry* (Hoff, A. J., Ed.) pp 707−752, Elsevier, Amsterdam.
26. Pascher, I., Lundmark, M., Nyholm, P.-G., and Sundell, S. (1992) *Biochim. Biophys. Acta 1113*, 339−373.
27. Ruocco, M. J., Siminovitch, D. J., Long, J. R., Das Gupta, S. K., and Griffin, R. G. (1996) *Biophys. J. 71*, 1776−1788.
28. Schroeder, R., London, E., and Brown, D. (1994) *Proc. Natl. Acad. Sci. U.S.A. 91*, 12130−12134.

BI000678R